Geometric Approach to Estimation of Volumetric Distortions

Alexander Naitsat[1], Emil Saucan[2] and Yehoshua Y. Zeevi[1]
[1]*Electrical Engineering Department, Technion, Haifa, Israel*
[2]*Max Planck Institute for Mathematics in the Sciences, Leipzig, Germany*

Keywords: Conformal Geometry, Isometric Distortion, Volume Parameterization, Volumetric Meshes, Geometric Computing, Computer Graphics.

Abstract: The problem of measuring geometrical distortions is not trivial for volumetric domains. There exist intrinsic restrictions and constrains on higher dimensional mappings. Moreover, according to Liouville theorem, most existing techniques for 2D data can not be directly applied to volumetric objects. In this work we approximate continuous deformations by piecewise affine functions defined on tetrahedral meshes. Our aim is to study a few types of geometrical distortions that can be expressed as functions of singular values of a Jacobian. We employ the proposed methods of estimating conformal and isometric distortions to analyze volumetric data. In particular, we examine parametrization of tetrahedral models to a ball. Distortions produced by the resulting spatial mappings depict intrinsic structure of domains, and therefore can be employed in such tasks as detection of abnormalities and comparison (i.e. similarity assessment) between 3D objects. This geometric approach and results are highly relevant to various applications in Computer Vision, Computer Graphics, 3D Printing and Medical Imaging.

1 INTRODUCTION

In mapping between volumetric domains, we are interested in quantifying distortions of the intrinsic geometrical properties, i.e. angles and Euclidean lengths, referred to as *conformal* and *isometric distortions*, respectively. Obeying the condition of angle preserving transformations, conformal maps are desirable in digital geometry processing and in computer graphics, since they do not exhibit shear and, therefore, preserve different vertex properties as well as the topology of the mesh itself. They are also instrumental in image processing and in computer vision.

A conformal mapping f of a domain $D \subset \mathbb{R}^n$ is defined as a smooth bijective function, which at any point $x \in D$ scales the space uniformly in every direction. This can be stated formally as

$$\|df_x \cdot h_1\| = \|df_x \cdot h_2\|, \tag{1}$$

where df_x denotes the Jacobian matrix at a point x of a function $f : D \to \mathbb{R}^n$ and $h_1, h_2 \in \mathbb{R}^n$ are arbitrary unit vectors. Following this annotation, a conformal map $f(x)$ is isometric in D if

$$\forall x \in D : |\det df_x| = 1. \tag{2}$$

Most of the methods used to construct conformal and almost isometric parametrization of a surface can't be generalized for dealing with volumes, due to the classical theorem of Liouville (Kühnel and Rademacher, 2007), which states that every conformal mapping of a domain in $\mathbb{R}^n, n \geq 3$, is a restriction of Möbius transformation, i.e. a composition of conformal affine transformations and inversions in a sphere. Therefore, the problem of computing perfect conformal functions in higher dimensions is reduced to minimizing the amount of distortion produced by a spatial mapping.

Conformal and isometric properties of smooth mappings in $\mathbb{R}^n$ can be studied by at least two alternative approaches. The first approach considers topological properties of a function along the integrable curves. The other approach, which we shall employ, examines the properties of a map in infinitely small neighborhoods. To this end, we examine the behavior of a discrete map f in nearest neighborhood represented by a ring of tetrahedral cells. Our measurements of distortions are based on the singular value analysis of the Jacobian df.

The advantage of this method over other techniques that are used in volumetric modeling (e.g. discrete harmonic energy; (Wang et al., 2003)) is that we can employ the same framework to deal with a wide range of spatial distortions and energies. For instance, the aspect-ratio distortion (Aigerman and Lip-

Naitsat, A., Saucan, E. and Zeevi, Y.
Geometric Approach to Estimation of Volumetric Distortions.
DOI: 10.5220/0005778201030110
In *Proceedings of the 11th Joint Conference on Computer Vision, Imaging and Computer Graphics Theory and Applications (VISIGRAPP 2016) - Volume 1: GRAPP*, pages 105-112
ISBN: 978-989-758-175-5

man, 2013), the certain types of rigid and affine energies (Kovalsky et al., 2014), the n-D comformality distortion (Lee et al., 2015), the angle and the volume energies (Paillé and Poulin, 2012) all of which are expressed as functions of singular values.

While there is an abundance of studies and applications of conformal mappings in 2D, general volumetric domains can be mapped only quasi-conformally. Therefore one of the challenges in 3D is to measure the minimal conformal distortion associated with mapping of one domain into another.

We examine the problem of measuring volumetric distortions, produced by discrete transformations between tetrahedral meshes, and addresses issues concerning relations between volumetric distortions and assessment of geometric similarity between 3D objects.

2 VOLUMETRIC DISTORTIONS

Let $f(x) = Ax + b$ be a full rank n-dimensional affine function. A number of geometry processing problems associated with f are naturally described in terms of singular values of its linear part. Singular values of a matrix are non-negative numbers usually denoted by $\sigma_1(A) \geq \sigma_2(A) \geq ... \geq \sigma_n(A)$; they are unique up to the order, and satisfy

$$\|A\| = \sigma_1,\ \ell(A) = \sigma_n,\ |\det A| = \prod_{i=1}^{n} \sigma_i, \tag{3}$$

where

$$\|A\| := \max_{\|h\|=1} \|A \cdot h\|, \tag{4}$$

is also known as the *spectral norm* of A, and

$$l(A) := \min_{\|h\|=1} \|A \cdot h\|. \tag{5}$$

The geometrical interpretation is that A transforms vectors of some unitary basis $\{v_i\}_{i=1,..,n}$ to the vectors of other unitary basis $\{u_i\}_{i=1,..,n}$, multiplied by the corresponding singular value σ_i. Putting these vectors in rows and columns, respectively, yields a singular value decomposition (SVD) of A

$$A = U \mathrm{Diag}(\sigma_1, ..., \sigma_n) V^*. \tag{6}$$

The latter plays an important role in image processing and numerical analysis.

When dealing with volumetric mappings, our primary interest is in studying distortions of first order differential properties, such as angles and Euclidean lengths. This lends itself to the definition of *qc* (quasi-conformal) and *qi* (quasi-isometric) dilatations of a linear map A, which basically are measures of how far A is from being conformal and isometric mapping, respectively. The basic method to assess the degree of conformality of a linear map A, is to consider the ratio of singular values

$$H(A) = \frac{\|A\|}{\ell(A)}, \tag{7}$$

also known as *the condition number*.

A more accurate approach, which follows from the theory of n-dimensional mappings, is to consider the following quantity, called *qc-dilatation*,

$$K(A) = \max\left\{ \frac{|\det(A)|}{\ell(A)^n}, \frac{\|A\|^n}{|\det(A)|} \right\}. \tag{8}$$

Quasi-isometric dilatation of a function f is defined as a minimal number $C \in \{1, \infty\}$, such that

$$\frac{1}{C}\|p_1 - p_2\| \leq \|f(p_1) - f(p_2))\| \leq C\|p_1 - p_2\|,$$

for any $p_1, p_2 \in D$ (see (Saucan et al., 2008)). In particular, for a linear function A, Eq. (4) and Eq. (5) imply

$$C(A) = \max\{\ell(A)^{-1}, \|A\|\}. \tag{9}$$

Dilatations defined above are related to each other via the following inequality

$$K(A) \leq H^{n-1}(A) \leq C^{2(n-1)}(A). \tag{10}$$

Now, suppose that f is a local diffeomorphism of an open domain $D \subset \mathbb{R}^n$, that is for each point in D there is a neighborhood where f is a smooth bijective mapping with a smooth inverse. We refer to such mapping simply as a *deformation function*. Clearly, df_x is a full rank linear transformation, and thus we define the *maximal qc-dilatation* of f as

$$K(f) = \sup_{x \in D} K(df_x), \tag{11}$$

and the *maximal qi-dilatation* as

$$C(f) = \sup_{x \in D} C(df_x). \tag{12}$$

We call a deformation function f *qc-mapping* if $K(f) < \infty$, and *qi-mapping* if $C(f) < \infty$.

In the sequel we shall assume that $n = 3$ and that all the above conditions for f are satisfied. The basic common method to represent volumetric data in computer science and engineering is to triangulate a continuous volume into tetrahedrons. This is a powerful method applicable for various 3D topologies. Employing this approach to approximate a continuous deformation $f : D \to D'$ yields the so-called simplicial map f_s.

Let (V, E, F, T) be a tetrahedral representation of D, where V, E, F and T are the vertex, edge, face

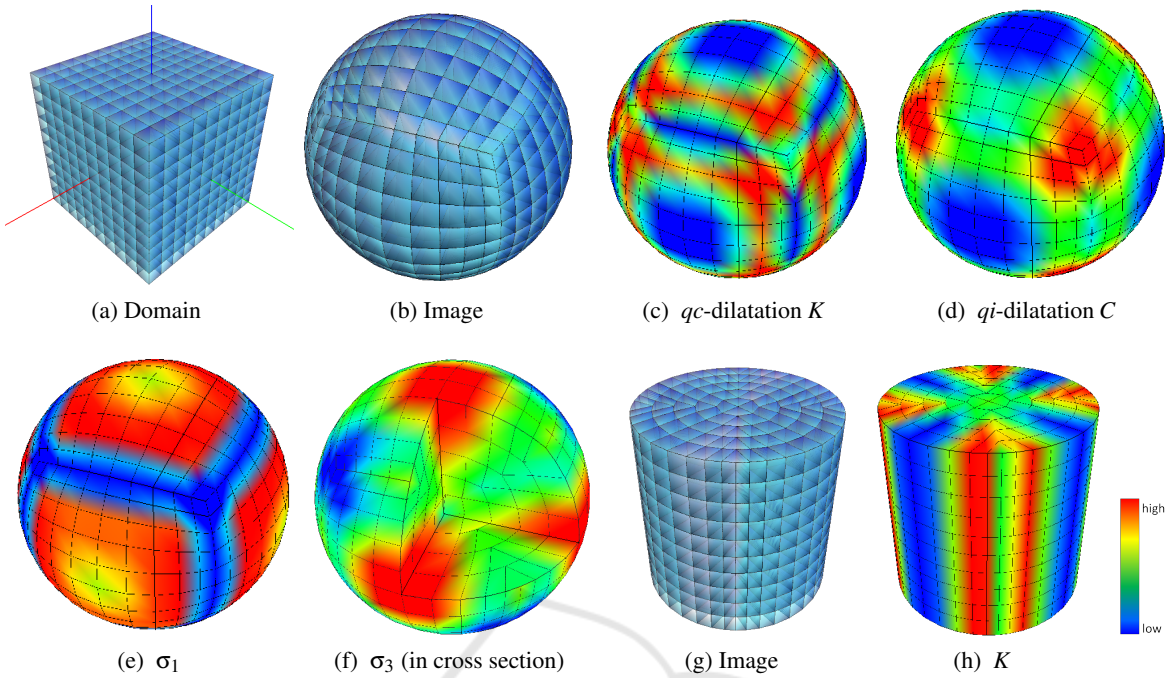

(a) Domain (b) Image (c) qc-dilatation K (d) qi-dilatation C

(e) σ_1 (f) σ_3 (in cross section) (g) Image (h) K

Figure 1: Radial stretching of the hexahedral volume of the cube $[-1,1]^3$ onto the unit ball and onto the round cylinder $\mathbb{B} \times [-1,1]$. Figures 1(c)-1(f) and 1(h) depict distribution diagrams of the scalar values associated with volumetric distortion: qc and qi dilatations and singular values σ_i of a Jacobian. Equivalent tetrahedral meshes are obtained by hexahedral triangulation.

and tetrahedra sets of the mesh, respectively. Then, for a vertex $v \in V$ located at the position x we set $f_s(v) = f(x)$. Next, we extent f_s to the entire domain by a piecewise linear extension of the vertex values (see the exact formula, Eq. (13)). The following section uses simplicial maps to estimate differential properties of continuous deformations.

2.1 Computing Singular Values

We can estimate dilatations of a simplicial map f at vertex v, placed at a position $x \in \mathbb{R}^3$, based on estimation of the Jacobian matrix df_x. First, we estimate the average Jacobian matrix inside a given tetrahedron τ, denoted by df_τ. Then we define the vertex Jacobian matrix df_v as an average over df_τ in the neighbouring tetrahedra.

Let $f^{(1)}, f^{(2)}, f^{(3)}$ be the coordinate components of the map f, where each one is a function from V to $\mathbb{R}$. We can express df_v as the matrix whose rows are the average gradient vectors of $f^{(i)}$.

Suppose $\boldsymbol{r}$ is a point inside tetrahedral cell τ, which consists of vertices v_1, v_2, v_3, v_4. Let λ_j be a face against v_j. Let $\boldsymbol{s}_j$ be the vector along the normal of λ_j, such that $\|\boldsymbol{s}_j\| = \mathrm{Area}(\lambda_j)$. If v_4 is set to be the origin of τ, then applying 3D barycentric coordinates for f yields

$$f^{(i)}(\boldsymbol{r}) = \frac{1}{3\mathrm{m}(\tau)} \sum_{j=1}^{4} (v_4 - \boldsymbol{r}) \cdot \boldsymbol{s}_j f^{(i)}(v_j). \qquad (13)$$

This implies that the gradient is constant inside τ, hence our estimates yield

$$\nabla f^{(i)}(\tau) = -\frac{1}{3\mathrm{m}(\tau)} \sum_{j=1}^{4} \boldsymbol{s}_j f^{(i)}(v_j); \qquad (14)$$

and

$$\nabla f^{(i)}(v) = \sum_{c \in \mathrm{Ring}(v)} \nabla f^{(i)}(c) w(c), \qquad (15)$$

where $\mathrm{Ring}(v)$ are the neighbouring tetrahedrons of v, and $w(c)$ are the chosen normalized weights.

The singular values $\sigma_1 = \|df_v\|$ and $\sigma_3 = l(df_v)$ are then approximated as the maximum and minimum of $\|df_v \cdot h_j\|$, sampled at chosen directions $h_1, \ldots, h_m$. The intermediate singular value is then

$$\sigma_2 = \frac{|\det(df_v)|}{\sigma_1 \sigma_3}, \qquad (16)$$

where the determinant can be computed directly from the estimates of the vertex Jacobian. Alternatively, it may be computed as a weighted average over determinants $\det(df_\tau)$, where the last quantity may be approximated as a volume ratio between the target and the source tetrahedra :

$$|\det(df_\tau)| = \frac{\mathrm{volume}\,(f(\tau))}{\mathrm{volume}\,(\tau)}. \qquad (17)$$

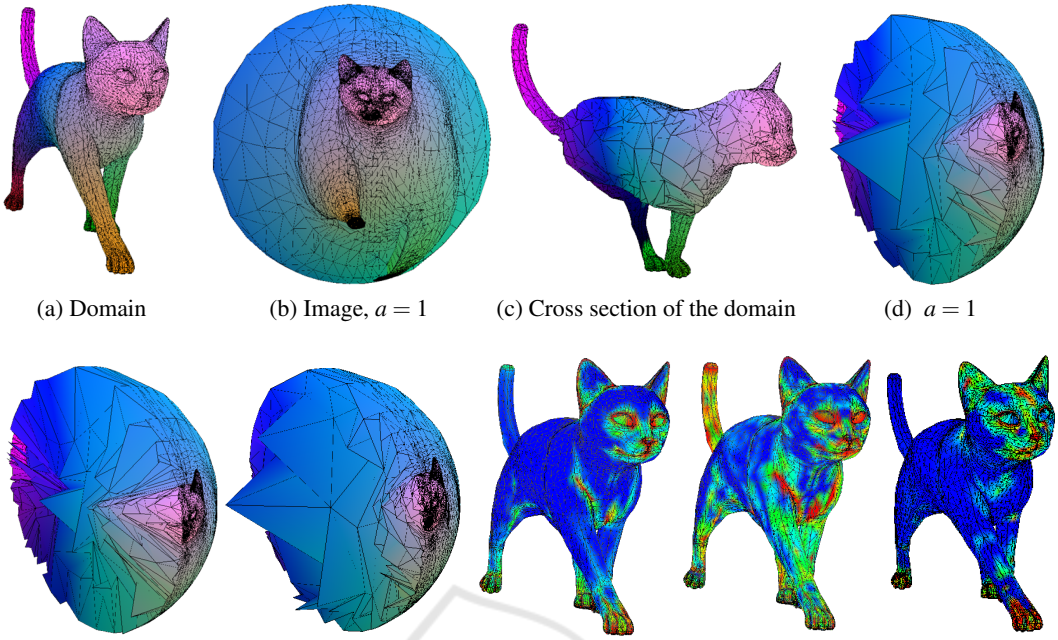

(a) Domain (b) Image, $a = 1$ (c) Cross section of the domain (d) $a = 1$

(e) $a = 2$ (f) $a = 0.5$ (g) Mean curvature (h) Dihedral angle (i) qc-dilatation

Figure 2: Parametrization of tetrahedral model mapped into a ball, computed for three different values of parameter a. Figures 2(a), 2(b) and 2(i) depict entire tetrahedral models of the domain and of the image. Figures 2(c)-2(f) show cross sections delineated by yz plane. Colors depict and correspond to diagrams of cylindrical coordinates of the domain for Figures 2(a)-2(f), and distribution diagrams of mean curvature and dihedral angles of the boundary and qc-dilations for Figures 2(g)-2(i), respectively.

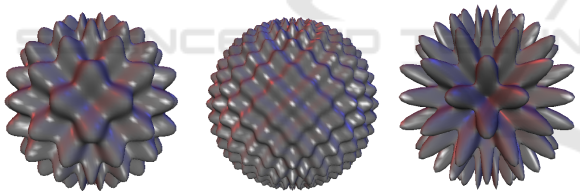

(a) $(0.2, 10)$ (b) $(0.1, 20)$ (c) $(0.5, 10)$

Figure 3: Images of the unit sphere under $\Omega_{A,\omega}$ functions. The shown pairs of numbers corresponds to the values of A and ω , respectively.

[See (Naitsat et al., 2015; Naitsat et al., 2014) for details about estimation of singular values and the Jacobian on tetrahedral and hexahedral meshes.]

Combining the above leads to numerical estimates of local volumetric distortions at vertex positions. We denote the corresponding qc and qi dilatations for a chosen vertex v by $K(f,v)$ and $C(f,v)$, respectively.

2.2 Bounded Distortion Mappings

A variety of techniques for morphing of polygonal meshes are used in computer graphics to measure similarities between objects. Let us consider the following related problem for volumetric domains.

Assume $D_1, D_2 \subset \mathbb{R}^3$ are smooth domains that have the same topology and similar geometrical properties. Then, according to the basic geometric intuition, there exists a deformation map $f : D_1 \mapsto D_2$ with bounded dilatations. The proof and exact conditions required for the existence can be found at (Caraman, 1974; Väisälä, 1971). We consider the minimal conformal and isomtertic distortions that are required to map one domain into another. The corresponding quantities are called *quasi-conformal* and *quasi-isometric coefficients* of D_1 and D_2, respectively, and they are defined as

$$K(D_1, D_2) = \inf K(f), \tag{18}$$

$$C(D_1, D_2) = \inf C(f), \tag{19}$$

where the infimum is taken over all smooth bijective mappings $f : D_1 \to D_2$.

We expect that the amount of distortion produced by morphing domain D_1 into D_2 will provide a measure of resemblance between their geometries. For instance, if D_2 is image of D_1 under a similarity transformation, then $K(D_1, D_2) = 1$. In a general case $K(D_1, D_2) \geq 1$ and it measures how close are these domains to being conformally-equivalent.

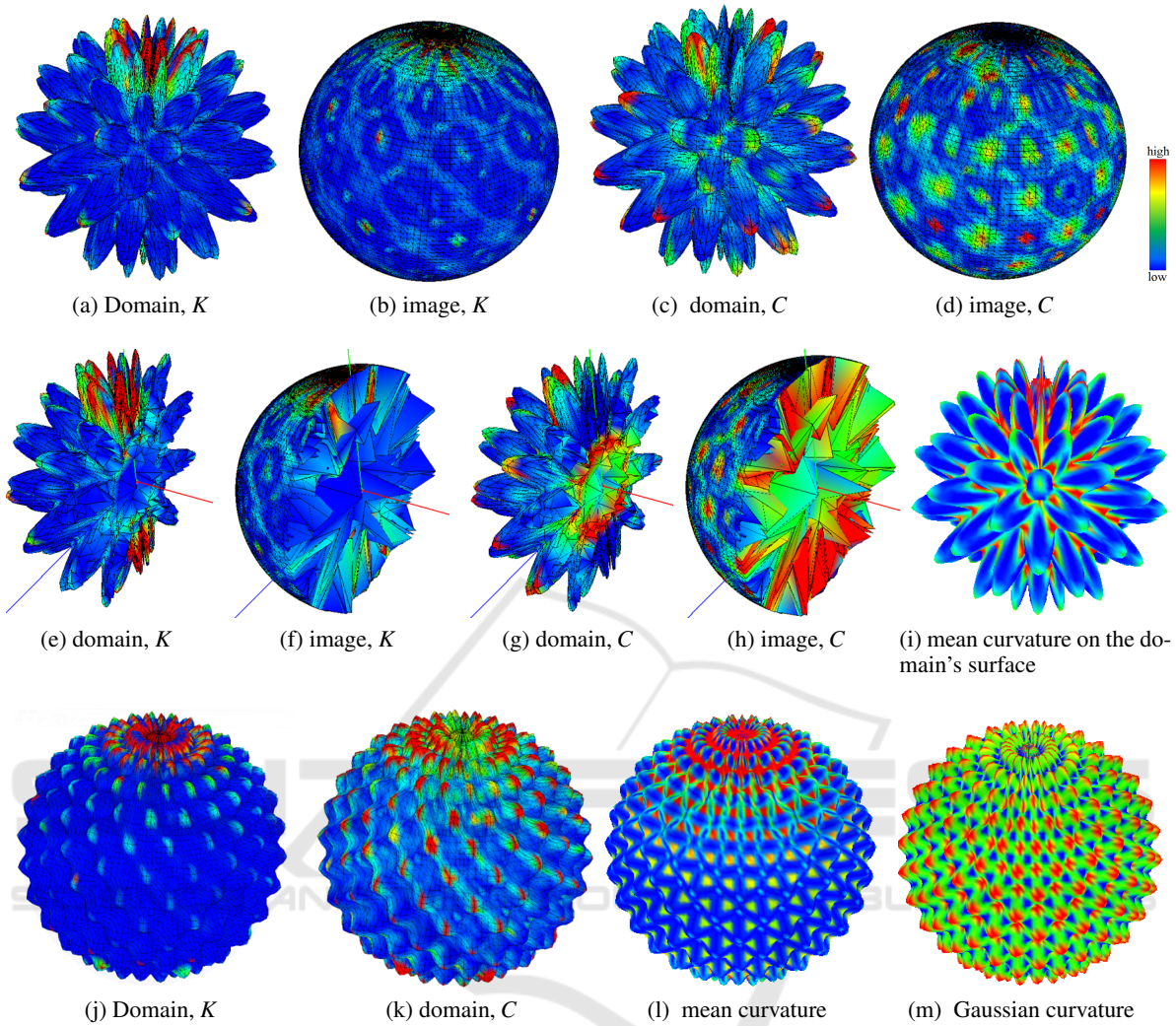

(a) Domain, K (b) image, K (c) domain, C (d) image, C

(e) domain, K (f) image, K (g) domain, C (h) image, C (i) mean curvature on the domain's surface

(j) Domain, K (k) domain, C (l) mean curvature (m) Gaussian curvature

Figure 4: Mapping into a ball of volumes contained inside the wave-like surfaces $\Omega_{A,\omega}(\mathbb{S}^3)$ defined by Eq. (25) for the following values of the amplitude A and the frequency ω : $A = 0.5, \omega = 10$ for Figures 4(a)-4(i) and $A = 0.1, \omega = 20$ for Figures 4(j)-4(m). The first two lines alternatively show domain and image of the deformation. Figures 4(a)-4(d) and 4(j)-4(k) show entire tetrahedral models, while 4(e)-4(h) depict cross sections. The rest of the Figures 4(i), 4(l) and 4(m) are diagrams of curvature distribution on boundary surfaces.

To access fine geometrical features of the object from *qi*-coefficients, we must take into account relative sizes of the given domains. Let us measure the size of a domain D_i by the radios r_i of the bounding sphere, i.e, the smallest sphere containing D_i. Given a deformation mapping $f : D_1 \to D_2$, it is often useful to consider the so called *k-bounded qi-dilation* of f

$$C'(f) = \frac{C(f)}{k}, \tag{20}$$

where k is defined by

$$k(D_1, D_2) = \max\left\{\frac{r_1}{r_2}, \frac{r_2}{r_1}\right\}. \tag{21}$$

We define the *k-bounded qi-coefficient* $C'(D_1, D_2)$ accordingly. This approach is important for a general case. However to make things simpler when dealing with tetrahedral models, we assume that $k(D_1, D_2) = 1$. This assumption is easily achieved in modeling tools by scaling the data during the preprocessing.

Dilatation coefficients can be often derived from comparison between domain's boundaries. For example, consider deformation of a cube onto the round cylinder shown in Figure 1. This transformation is a radial stretching of the square in planes $\mathbb{R}^2 \times \{z\}$, with edge $2l$ into the circle of radius l, which can be written explicitly in cylindrical coordinates as

$$(r, \varphi, z) \mapsto \left(\frac{lr}{R(\varphi)}, \varphi, z\right), \tag{22}$$

where $R(\varphi)$ is a distance from the origin to the boundary of the cube, measured at angle φ. Without loss of generality, we focus on compact domains in $\mathbb{R}^3$ with non-empty interior that contains the origin.

The mapping (22) for $l = 1$ can be generalized to construct parametrization of compact volumes onto the unit cylinder by

$$(r,\varphi,z) \mapsto \left(\left(\frac{r}{R(\varphi)} \right)^a, \varphi, z \right), \qquad (23)$$

where $a > 0$ is a chosen parameter.

The same technique of radial stretching can be applied to produce volumetric parametrization into the unit ball. Consider a domain D that satisfies the following geometrical condition: for any $\zeta \in \partial D$, the angle between the line segment $\overline{\zeta 0}$ and tangent plane at ζ is larger than or equal to some constant $\alpha > 0$. We construct a smooth parametrization of D into the unit ball written in the spherical coordinates (r,φ,θ). First, set $\zeta(\varphi,\theta)$ to be the furthest intersection point of ∂D and the ray along the φ,θ direction, then we define the family of parametrization functions $f_a : D \to \mathbb{B}^3$ by

$$(r,\varphi,\theta) \mapsto \left(\left(\frac{r}{\|\zeta(\varphi,\theta)\|} \right)^a, \varphi, \theta \right), \qquad (24)$$

where $a > 0$ is the same parameter as in Eq. (23).

If the domain is star-shaped, namely if for any $x \in D$: $\overline{0x} \subset D$, then the resulting parametrization is onto.

Moreover, Caraman (Caraman, 1974, p. 408) has shown in this case that f_a is a qc-mapping and gave an accurate approximation of $K(f_a)$ as a function of a and angle α from the geometrical condition. In particular, if $a \to 1$ and $\alpha \to \pi/2$, then $K(f_a)$ approaches 1, since the limit function appears to be a uniform scaling of a ball to the unit ball $\mathbb{B}^3$.

Figures 1 and 2 show cylindrical and spherical parametrization of models. Both parametrizations applicable to analysis of volumetric data. However, parametrization to a cylinder requires an accurate choice of the rotation axis, where deformation to a ball is invariant to the initial orientation of objects. Therefore, this work is focused on radial stretching into a ball. Figures 2(a)-2(f) depict the geometrical meaning of the parameter a, which affects the amount of distortion along the radial axis. In particular, when a decreases, the interior volume is stretched toward the surface, while raising values of a squeezes the interior toward the origin. This behavior can be employed to adjust the amount of local distortions. In the sequel we assume $a = 1$, unless stated otherwise.

2.3 Results and Explanations

We present results of numerical computations of volumetric distortions for various domains along with the qualitative interpretation of the outcomes.

Figure 2 summarizes results for the parametrization of the cat model to the unit ball, represented by a tetrahedral mesh. Note the correlation between areas on the surface of higher values of dilatations and areas of higher values of mean curvature and dihedral angles shown in Figures 2(g) and 2(h). This phenomenon is further emphasized in Figure 4. The relation between curvature and measured volumetric distortions follows from the existence of conformal and isometric invariants. Similarly, dihedral angle imposes tight bounds on qc-coefficients of polyhedral domains. These facts has been demonstrated for basic deformations in (Naitsat et al., 2015).

Next, we choose series of symmetrical volumetric domains $D_{A,\omega}$ whose boundaries $\partial D_{A,\omega}$ are set to be an image of the following wave functions:

$$\Omega_{A,\omega}(r,\varphi,\theta) = (r + A\cos(\omega\varphi)\cos(\omega\theta), \varphi, \theta), \qquad (25)$$

where r is a constant. In other words, we define a sinusoid height function on a sphere $\mathbb{S}^3_r$ with amplitude A and frequency ω (see Figure 3). Our aim is to estimate an impact that distinct geometrical features of a wavelike surface have on the dilatation coefficients. Although, Eq. (11) and Eq. (12) define $K(f)$ and $C(f)$ as a maximum of the corresponding local dilations, the average value of the volumetric distortion is more relevant for such practical applications as shape classification and comparison. Let us denote the average value of a scalar function $F : D \subset \mathbb{R}^3 \to \mathbb{R}$ by

$$\bar{F} = \frac{1}{\text{volume}(D)} \int_D F(\boldsymbol{x}) d\boldsymbol{x} \qquad (26)$$

In order to compute $\bar{K}$ and $\bar{C}$ for a tetrahedral mesh (V,E,F,T) of a domain D, we approximate continuous integration as follows :

$$\int_D F(\boldsymbol{x})\, d\boldsymbol{x} \approx \sum_{v \in V} F(v) \cdot \text{volume}(\text{Cent}(v)), \qquad (27)$$

where $\text{Cent}(v)$ is a *barycentric cell* of a vertex v, obtained by connecting middle points of edges sharing v. Namely, for each $\tau \in \text{Ring}(v)$ we construct a sub-tetrahedron by connecting v and middle points of edges sharing v. $\text{Cent}(v)$ is defined as the union of these sub-tetrahedrons over $\text{Ring}(v)$.

Denote by $D_{A,\omega}$ the volume enclosed by the images of the unit sphere under $\Omega_{A,\omega}$. Figure 4 considers deformations $f_1 : D_{A,\omega} \to \mathbb{B}^3$ defined by Eq. (24). Observing these figures, we see concentration of conformal distortion on the surface of the model, while isometric distortion is spread through the entire volume. The phenomenon is related to the choice of a deformation function f_1 from Eq. (24) which is a uniform scaling when restricted to a radial segment $\{(r,\varphi,\theta) | r \in [0,t]\}$.

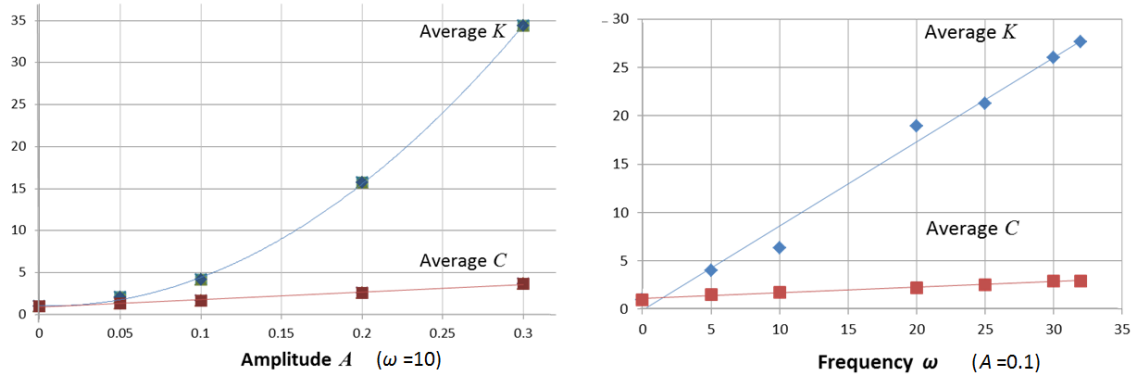

Figure 5: Average *qi* and *qc* dilatations $\bar{K}$ and $\bar{C}$ as a function of the amplitude A and the frequency ω of $\Omega_{A,\omega}$ defined according to Eq. (25). Dilatations are computed for parametrization (24) of domains $D_{A,\omega}$, which are interior volumes of $\Omega_{A,\omega}(\mathbb{S}^3)$. The results are shown for the constant frequency $\omega = 10$ and the constant amplitude $A = 0.1$, respectively.

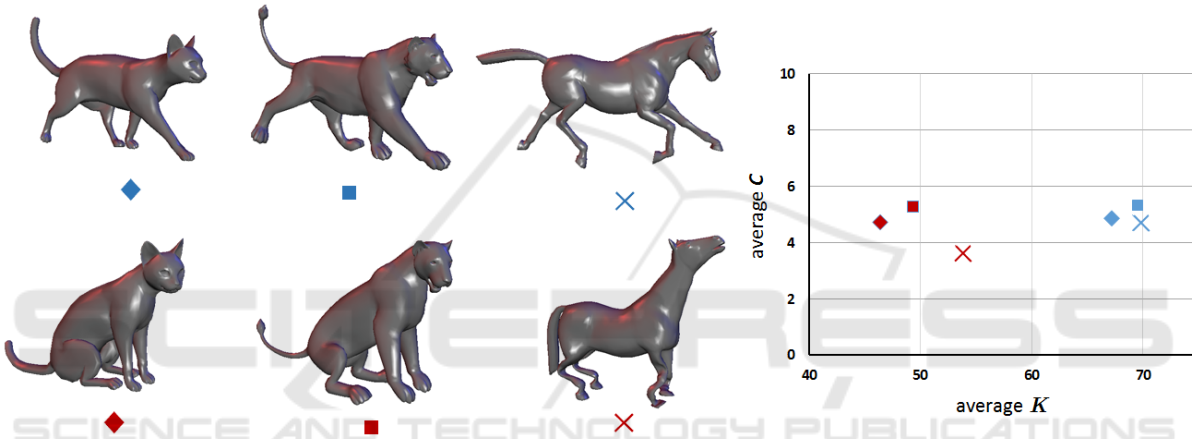

Figure 6: Average volumetric distortions $\bar{K}$ and $\bar{C}$ produced by parametrization of 3D models into a ball. The corresponding distances between models in $(\bar{K},\bar{C})$-plane reveal similarities of global geometrical features. The mesh data used in this simulation was adopted from (Sumner and Popović, 2004).

The corresponding charts in Figure 5 show dependence between the wave parameters and the average level of volumetric distortions. As expected, for $\omega = \text{const}$, we see that $\bar{C}$ has a linear dependence on the amplitude, while $\bar{K}$ appears to be a quadratic function of A. In contrast, when the amplitude is constant, both $\bar{C}$ and $\bar{K}$ are nearly linear functions of ω. This is because conformal distortion is intensified near the surface, which for $A = \text{const}$ is restrained to the same area $1 - A \le r \le 1 + A$. 3D shapes can be analyzed in the spectral domain as a composition of components that represent features of high and low frequencies. These features can be estimated by the amount of distortion required to round the shape. This concept is illustrated in Figure 6 for three pairs of polygonal models. All the pairs, except the last one, are mutual images under a nearly isometric bending. Average distortions are measured and displayed on the $(\bar{K},\bar{C})$-plane for a deformation map (24) of the enclosed volumes into a ball. The vertical displacement of the resulting points in the distortion plane reveals how far are shapes from being isometrically equivalent, while the Euclidean distance between the points accesses the resemblance of global features and alignment of objects' medial axes.

3 CONCLUSIONS

This paper presents quantitative method of computing the major volumetric distortion: *qc* and *qi* dilatations. Our technique is based on estimation of the Jacobian and the corresponding singular values for a simplicial map.

Among other applications, our approach can be used to produce desirable deformations and parameterizations of 3D domains, by minimizing the distortion functional

$$\sum_{v \in V} K(f,v) + \lambda C(f,v), \qquad (28)$$

under the given conditions. The latest research in the area (Kovalsky et al., 2014), deals with the minimization of the condition number (7), which is not always sufficiently accurate to properly measure deformations in 3D (see (Naitsat, 2015, p. 13)). We believe that using our metrics it is possible to achieve more desirable results.

We have demonstrated in Section 2.2 basic parametrization techniques for volumetric objects. Dilatations produced by the corresponding mappings are tightly related to the distortion of several geometrical properties of a boundary surface, such as curvature and dihedral angles. In particular, we have illustrated in Section 2.3 correlations between an average distortion, the amplitude and the frequency of wave-like surfaces. These consequences may be targeted toward spectral analysis of the closed shapes that can be represented as an image of a sphere under a composition

$$\Omega_{A_1,\omega_1} \circ \Omega_{A_2,\omega_2} \circ \dots , \tag{29}$$

which can be considered, in turn, as an analogue of Fourier series in the spherical coordinates. Likewise, future analysis may consider distortions produced by parametrization into non-symmetrical domains and its relation to global properties of shapes. For example, a volumetric parametrization into cylinder and shape's symmetry relative to the rotation axis.

As has been illustrated in Figure 6, these facts can be instrumental in quantitative assessment of similarity of objects undergoing elastic deformations. Unlike most existing algorithms for classification and comparison of polygonal meshes, our approach can be applied both for closed simply-connected surfaces and for volumetric domains with more sophisticated boundaries.

ACKNOWLEDGEMENTS

This research has been supported by the Israeli Ministry of Economics; OMEK consortium and by the Ollendorff Minerva Center for Vision and Image Sciences.

REFERENCES

Aigerman, N. and Lipman, Y. (2013). Injective and bounded distortion mappings in 3D. *ACM Trans. Graph*, 32(4):106:1–106:14.

Caraman, P. (1974). *n-dimensional quasiconformal (QCF) mappings. Revised, enlarged and translated from the Roumanian by the author.* Editura Academiei Române, Bucharest, Abacus Press, Tunbridge Wells Haessner Publishing, Inc., Newfoundland, NJ, 1974.

Kovalsky, S. Z., Aigerman, N., Basri, R., and Lipman, Y. (2014). Controlling singular values with semidefinite programming. *ACM Transactions on Graphics (TOG)*, 33(4):68.

Kühnel, W. and Rademacher, H.-B. (2007). Liouville's theorem in conformal geometry. *Journal de mathématiques pures et appliquées*, 88(3):251–260.

Lee, Y. T., Lam, K. C., and Lui, L. M. (2015). Landmark-matching transformation with large deformation via n-dimensional quasi-conformal maps. *J. Sci. Comput. (Accepted for publication)*, pages 1–29.

Naitsat, A. (2015). Quasi-conformal mappings for volumetric deformations in geometric modeling. Master's thesis.

Naitsat, A., Saucan, E., and Y, Y. Z. (2014). Computing quasi-conformal maps in 3d with applications to geometric modeling and imaging. In *2014 IEEE Convention, Israel*, pages 1–5.

Naitsat, A., Saucan, E., and Zeevi, Y. Y. (2015). Volumetric quasi-conformal mappings - quasi-conformal mappings for volume deformation with applications to geometric modeling. In *Proceedings of VISIGRAPP 2015*, pages 46–57.

Paillé, G.-P. and Poulin, P. (2012). As-conformal-as-possible discrete volumetric mapping. *Computers & Graphics*, 36(5):427–433.

Saucan, E., Appleboim, E., Barak-Shimron, E., Lev, R., and Zeevi, Y. Y. (2008). Local versus global in quasi-conformal mapping for medical imaging. *Journal of Mathematical Imaging and Vision*, 32(3):293–311.

Sumner, R. W. and Popović, J. (2004). Deformation transfer for triangle meshes. *ACM Transactions on Graphics (TOG)*, 23(3):399–405.

Väisälä, J. (1971). *Lectures on n-Dimensional Quasiconformal Mappings*. Springer-Verlag Berlin Heidelberg New York.

Wang, Y., Gu, X., Yau, S.-T., et al. (2003). Volumetric harmonic map. In *Communications in Information & Systems*, volume 3, pages 191–202. International Press of Boston.